

## LEPTOPRODUCTION OF SUPERSYMMETRIC PARTICLES

S.K. JONES and C.H. LLEWELLYN SMITH

*Department of Theoretical Physics, University of Oxford, 1 Keble Road, Oxford, UK*

Received 22 November 1982

We study the production of scalar leptons ( $\tilde{\ell}$ ), scalar quarks ( $\tilde{q}$ ) and gluinos ( $\tilde{g}$ ) in  $ep \rightarrow \tilde{\nu}X$ , and  $ep \rightarrow \tilde{e}X$  and the associated production of  $\tilde{q}$  and  $\tilde{g}$  in  $ep \rightarrow eX$  and  $ep \rightarrow \nu X$ . We find that  $\tilde{\nu}\tilde{q}$  and  $\tilde{e}\tilde{q}$  production is probably measurable at HERA for masses of order 40 GeV with exchanged particle masses of order 80 GeV. We derive and solve the asymptotic supersymmetric evolution equations for quark, gluon, scalar quark and gluino distributions. We find sum rules for the asymptotic momentum fractions and for the partition of the net quark number between quarks and scalar quarks. We use a fusion model to study associated leptoproduction in the threshold region. The only appreciable contribution is from small  $Q^2$  electroproduction but the rates are low even for scalar quarks and gluinos with masses close to the present limits.

### 1. Introduction

Interest in supersymmetry (SUSY) is enhanced by the belief that some SUSY particles may be light enough to be discovered at LEP, HERA or the  $p\bar{p}$  collider (for phenomenologically orientated reviews of SUSY and references see, e.g., ref. [1]). Most previous work on the production of SUSY particles has concentrated on  $e^+e^-$  annihilation [1, 2] and hadronic collisions [1, 3]. In this paper we analyse the production of SUSY particles in  $ep$  collisions at machines such as HERA through the following.

- (i) The fusion of an electron and quark to form a scalar lepton (slepton),  $\tilde{\ell}$ , and a scalar quark (squark),  $\tilde{q}$ :  $eq \rightarrow \tilde{\ell}\tilde{q}$ .
- (ii) The pair production of scalar quarks and gluinos ( $\tilde{g}$ ):  $eq \rightarrow e[\nu]\tilde{q}\tilde{g}$  and  $eg \rightarrow e[\nu]\tilde{q}\tilde{q}$ .

We also discuss the influence of scalar quarks and gluinos on the evolution of deep inelastic structure functions. The influence of light gluinos has been calculated previously [4], including second order corrections [5]. As far as we are aware, the only other detailed work on SUSY lepto-production is a calculation [6] of the production of a scalar lepton plus a spinor  $W$  or  $Z$ .

The strong coupling of scalar quarks and gluinos are fixed in SUSY QCD, as are the electroweak couplings of the gauge spinors ( $\tilde{W}, \tilde{B}$ ) in SUSY  $SU(2) \times U(1)$ . The only unknowns which enter the cross sections we consider are:

- (a) the masses;
- (b) the mixing between  $\tilde{W}^0$  and  $\tilde{B}$  to form mass eigenstates;

(c) the coupling of the goldstino ( $\tilde{G}$ ) – the Goldstone fermion generated by the spontaneous breaking of SUSY – which depends on the scale at which SUSY is broken.

Experimentally, scalar quarks and charged scalar leptons must be heavier [7] than 15 GeV and gluinos must be heavier [3] than a few GeV. Theoretical expectations for the mass spectrum are very uncertain but fall into two classes.

(i) In D-type models [8] the scalar quarks and leptons typically have masses less than  $M_w$  (e.g. in Fayet's model [8] they are bounded by  $\frac{1}{2}M_w$ ) and the mass of the gluino is a few GeV. The gauge spinor mixing angles are essentially the same as the vector boson mixing angles i.e. the mass eigenstates are the photino  $\tilde{\gamma}$  and  $\tilde{Z}$  – the spinor  $Z^0$ . The lightest SUSY particles are the massless Goldstino and the (very light) photino. Scalar quarks decay rapidly to  $q + \tilde{G}$ . The gluino decays to  $g + \tilde{G}$  or  $q\bar{q}\tilde{\gamma}$ , the latter mode being dominant if the scale of SUSY breaking  $\Lambda_{ss}$  is greater than  $11 m_{\tilde{q}}$  as discussed by Kane and Leveille [3].

(ii) In F-type models [9] a typical mass spectrum [10] is

$$\tilde{H}^0 \ll \tilde{H}^\pm \ll \tilde{B} \ll \tilde{\ell} = W(?) < \tilde{W} < \tilde{q} < \tilde{g} \text{ (few TeV)},$$

where  $\tilde{H}$  are spinor Higgs particles. In these models  $\Lambda_{ss}$  may well be much greater than  $10^6$  GeV in which case the Goldstino effectively decouples i.e. the lifetime for SUSY particles which could be produced at HERA to decay into  $\tilde{G}$  is such that they would escape the detector before decaying. Decays can proceed directly to the ground state

$$\tilde{\ell}, \tilde{q}, \tilde{g} \rightarrow \ell, q, g + \tilde{H}^0.$$

However, they may also proceed via a second  $H^0$  which is expected to be not much heavier than  $\tilde{H}^0$

$$\begin{aligned} \tilde{\ell}, \tilde{q}, \tilde{g} &\rightarrow \ell, q, g + \tilde{H}^0 \\ &\quad \downarrow \\ &\quad \tilde{H}^0 + \bar{\ell}\ell, \end{aligned}$$

or via an  $\tilde{H}^\pm$  which decays to  $\tilde{H}^0 + e\nu, \mu\nu, \tau\nu$ .

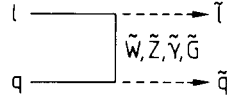
There is little hope of finding SUSY particles at HERA if they have the masses suggested by F-type models. However, if the masses are less, the F-type decays provide excellent signatures which would make it possible to detect processes with very low rates. While bearing this in mind, our discussion is based on the D-type decays  $\tilde{q} \rightarrow q + \tilde{G}$ ,  $\tilde{g} \rightarrow g + \tilde{G}$  relying on missing energy-momentum for a signature.

This paper is organised as follows. In sect. 2 we discuss the process  $eq \rightarrow \tilde{\ell}\tilde{q}$ . In sect. 3 we derive the asymptotic evolution equations for SUSY QCD and give the solutions for the singlet momentum fractions and non-singlet number fractions. The results of these evolution calculations suggest that it might not be impossible to detect leptonproduction of pairs of SUSY particles at HERA. However, in using the evolution equations we simply switch on the contribution of SUSY particles at

a threshold in  $Q^2$  beyond which they are treated as massless. This gives the correct behaviour to leading order in  $\alpha_s$ , well beyond threshold, but is quite unreliable in the threshold region. We therefore turn to the fusion model which, as discussed in sect. 4, should be reliable in the threshold region, to make realistic estimates of production cross sections at HERA energies. Our conclusions are summarised in sect. 5. In an appendix, we record the Feynman rules for Majorana particles which are needed in our calculations; although quite straightforward to derive, they have not appeared explicitly in the literature as far as we are aware.

## 2. Direct production of a slepton plus squark

A lepton and quark can fuse to produce scalar particles thus:



In the case of charged  $\tilde{W}^\pm$  exchange the differential cross section for left/right handed incident leptons and quarks is

$$\begin{aligned} \frac{d\sigma_{RR}^{LL}}{dt} &= \left( \frac{e}{\sin \theta} \right)^4 \frac{1}{16\pi\hat{s}} \left( \frac{\mu}{t-\mu^2} \right)^2, \\ \frac{d\sigma_{RL}^{LR}}{dt} &= \left( \frac{e}{\sin \theta} \right)^4 \frac{1}{16\pi\hat{s}^2} \frac{[-(M_1^2 - t)(M_2^2 - t) - \hat{s}t]}{(t - \mu^2)^2}, \end{aligned} \quad (1)$$

where  $\hat{s}$  is the lepton-quark c.m. energy squared,  $\mu$  the mass of the exchanged particle and  $M_{1,2}$  the masses of the slepton and squark. We assume that the scalars and pseudoscalars are degenerate. In the case of squarks, large mass splittings are ruled out [11] by limits on  $\Delta S = 0$  parity-violating amplitudes. The total cross sections are given by

$$\sigma^{AB} = \left( \frac{e}{\sqrt{2} \sin \theta} \right)^4 \hat{\sigma}^{AB}(\mu), \quad (2)$$

where

$$\begin{aligned} \hat{\sigma}_{RR}^{LL}(\mu) &= \frac{1}{4\pi\hat{s}} \frac{\mu^2 \chi}{(\mu^2 - M_1^2)(\mu^2 - M_2^2) + \hat{s}\mu^2}, \\ \hat{\sigma}_{RL}^{LR}(\mu) &= \frac{1}{4\pi\hat{s}^2} \left[ (2\mu^2 + \hat{s} - M_1^2 - M_2^2) \ln \left( \frac{\hat{s} + 2\mu^2 - M_1^2 - M_2^2 + \chi}{\hat{s} + 2\mu^2 - M_1^2 - M_2^2 - \chi} \right) - 2\chi \right], \end{aligned} \quad (3)$$

with

$$\chi = \sqrt{(\hat{s} - M_1^2 - M_2^2)^2 - 4M_1^2 M_2^2}.$$

In the case of neutral currents we do not give the differential cross section explicitly as it can be constructed from (1) and the equations below. The total cross section is given by

$$\sigma^{\text{AB}} = \sum_i (C_i^{\text{AB}})^2 \hat{\sigma}^{\text{AB}}(\mu_i) + \sum_{i \neq j} C_i^{\text{AB}} C_j^{\text{AB}} \hat{\sigma}_{\text{int.}}^{\text{AB}}(\mu_i, \mu_j), \quad (4)$$

where  $i$  and  $j$  run over the neutral mass eigenstates and

$$\begin{aligned} \hat{\sigma}_{\text{int.}}^{\text{LL}}(\mu_i, \mu_j) &= \frac{\mu_i \mu_j}{2\pi \hat{s}(\mu_i^2 - \mu_j^2)} \\ &\times \left[ \ln \left( \frac{\hat{s} + 2\mu_j^2 - M_1^2 - M_2^2 + \chi}{\hat{s} + 2\mu_j^2 - M_1^2 - M_2^2 - \chi} \right) - (i \leftrightarrow j) \right], \\ \hat{\sigma}_{\text{int.}}^{\text{LR}}(\mu_i, \mu_j) &= \frac{-1}{2\pi \hat{s}^2} \left[ \chi + \left( \mu_j^2 \hat{s} + \frac{(\mu_j^2 - M_1^2)(\mu_j^2 - M_2^2)}{(\mu_i^2 - \mu_j^2)} \right) \right. \\ &\times \ln \left( \frac{\hat{s} + 2\mu_j^2 - M_1^2 - M_2^2 + \chi}{\hat{s} + 2\mu_j^2 - M_1^2 - M_2^2 - \chi} \right) + (i \leftrightarrow j) \left. \right]. \end{aligned} \quad (5)$$

In the case that the  $\tilde{\gamma}$  and  $\tilde{Z}$  are the mass eigenstates the couplings are given by

$$\begin{aligned} C_{\tilde{\gamma}}^{\text{AB}} &= -e^2 Q_q, \\ C_{\tilde{Z}}^{\text{AB}} &= \frac{e^2 (I_3^{\text{A}} - Q \sin^2 \theta)_e (I_3^{\text{B}} - Q \sin^2 \theta)_q}{\sin^2 \theta \cos^2 \theta}, \end{aligned} \quad (6)$$

whereas if the unmixed SU(2) and U(1) gauge spinors,  $\tilde{W}_3$  and  $\tilde{B}$ , are mass eigenstates

$$\begin{aligned} C_{\tilde{W}_3}^{\text{AB}} &= \frac{e^2}{\sin^2 \theta} (I_3^{\text{A}})_e (I_3^{\text{B}})_q, \\ C_{\tilde{B}}^{\text{AB}} &= \frac{e}{\cos^2 \theta} (Q - I_3^{\text{A}})_e (Q - I_3^{\text{B}})_q. \end{aligned} \quad (7)$$

In either case the Goldstino couplings are given by

$$\begin{aligned} C_{\tilde{G}}^{\text{AB}} &= \eta^{\text{AB}} \left( \frac{\Delta m_{\text{e}}^2}{d} \right) \left( \frac{\Delta m_{\text{q}}^2}{d} \right), \\ \eta^{\text{AB}} &= +1 \text{ for LL, RR,} \\ &= -1 \text{ for LR, RL,} \\ \Delta m^2 &= (\text{scalar mass})^2 - (\text{fermion mass})^2. \end{aligned} \quad (8)$$

where  $d = \Lambda_{\text{ss}}^2$  plays the role for spontaneously broken SUSY which  $f_\pi$  plays for spontaneously broken chiral symmetry and the couplings are determined by current

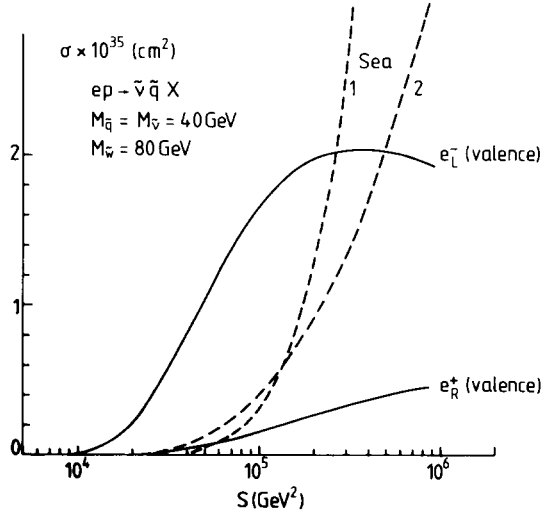


Fig. 1. Cross section for the electroproduction of a scalar neutrino ( $\tilde{\nu}$ ) and a scalar quark ( $\tilde{q}$ ) as a function of the c.m. energy squared for  $M_{\tilde{\nu}} = M_{\tilde{q}} = 40$  GeV,  $M_{\tilde{w}} = 80$  GeV. The contribution of the “sea” is shown for the distribution (1) of Owens and Reya (2) of Glück, Hoffman and Reya.

algebra [12]. It is known from astrophysical considerations [13] that  $A_{ss}$  is greater than 51 GeV but it is much larger in most models.

We construct electron-proton cross sections from electron-quark cross sections by folding with quark distributions  $q(x, Q^2)$ , where we take – somewhat arbitrarily:

$$Q^2 = \frac{1}{2}(|t_{\min}| + |t_{\max}|) = \frac{1}{2}(\hat{s} - M_1^2 - M_2^2). \quad (9)$$

We give results calculated using the quark and gluon distributions of Glück, Hoffman and Reya [14] (GHR). For comparison, we also give some results based on the distributions of Owens and Reya [15] (OR), which are very similar for the valence quarks but have a faster evolving sea contribution. The difference of the results provides an indication of the errors.

Some results for the charged current process  $eq \rightarrow \tilde{\nu}X$  are shown in fig. 1. For this figure we see that for  $M_{\tilde{w}} = 80$  GeV,  $M_{\tilde{q}} = M_{\tilde{\nu}} = 40$  GeV,  $s = 10^5$  GeV<sup>2</sup> (approximately the c.m. energy squared of the proposed HERA machine):

$$\begin{aligned} \sigma(e_L^- \rightarrow \tilde{\nu}) &= \left(1.7 + \begin{pmatrix} 0.3 \\ 0.4 \end{pmatrix}\right) \times 10^{-35} \text{ cm}^2, \\ \sigma(e_R^+ \rightarrow \tilde{\nu}) &= \left(0.15 + \begin{pmatrix} 0.3 \\ 0.4 \end{pmatrix}\right) \times 10^{-35} \text{ cm}^2, \end{aligned} \quad (10)$$

where the first contributions are due to valence quarks and the second the sea part for the OR (upper) and GHR (lower) distribution. We also considered the case

$M_{\tilde{W}} = 80 \text{ GeV}$ ,  $M_{\tilde{\nu}} = M_{\tilde{q}} = 20 \text{ GeV}$  for which we found

$$\begin{aligned}\sigma(e_L^- \rightarrow \tilde{\nu}) &= \left(4.7 + \binom{5.2}{2.8}\right) \times 10^{-35} \text{ cm}^2, \\ \sigma(e_R^+ \rightarrow \tilde{\nu}) &= \left(0.4 + \binom{5.2}{2.8}\right) \times 10^{-35} \text{ cm}^2,\end{aligned}\quad (11)$$

still for  $s = 10^5 (\text{GeV})^2$ , and  $M_{\tilde{W}} = 200 \text{ GeV}$ ,  $M_{\tilde{\nu}} = 40 \text{ GeV}$ ,  $M_{\tilde{q}} = 100 \text{ GeV}$  for which

$$\begin{aligned}\sigma(e_L^- \rightarrow \tilde{\nu}) &= \left(1.3 + \binom{0.02}{0.06}\right) \times 10^{-36} \text{ cm}^2, \\ \sigma(e_R^+ \rightarrow \tilde{\nu}) &= \left(0.02 + \binom{0.02}{0.06}\right) \times 10^{-36} \text{ cm}^2.\end{aligned}\quad (12)$$

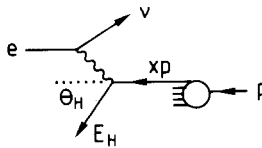
We found that these results can be scaled to other energies and masses quite accurately using

$$\sigma(\lambda s, \lambda M_i^2, \lambda \mu^2) \approx \lambda^{-1} \sigma(s, M_i^2, \mu^2), \quad (13)$$

which would be exact in the absence of QCD scaling violations.

With a luminosity of  $10^{31} \text{ cm}^{-2} \text{ sec}^{-1}$  (less by a factor of 6 than the luminosity hoped for at HERA [16]) a cross section of  $10^{-35} \text{ cm}^2$  gives 10 events per day. If  $\tilde{\nu}$  decays lead to a jet of charged leptons with a significant branching ratio it might be possible to detect  $e^- p \rightarrow \tilde{\nu} X$  down to the  $10^{-36} \text{ cm}^2$  level. However, as discussed in the introduction, such decays are only likely to occur in F-type models in which  $\tilde{\nu}$  and  $\tilde{q}$  are probably very heavy. In D-type models the favoured decay is  $\tilde{\nu} \rightarrow \nu \tilde{G}$ , in which case the events are indistinguishable from ordinary  $e^- p \rightarrow \nu X$  events, for which the cross section is approximately  $1.2 \times 10^{-34} \text{ cm}^2$  at  $s = 10^5 \text{ GeV}^2$  for left-handed electrons. For the case in eq. (11), the increase of the total cross section associated with the SUSY threshold would provide a clear signature at HERA. The O(20%) increase corresponding to eq. (10) might also be detectable.

The signal/noise can be enhanced, making heavier masses detectable, by making suitable cuts. Recall that in ordinary charged current events the kinematic variables  $x$  and  $y$  can be reconstructed approximately from the observed hadrons using the naive parton model and assuming no missing neutral energy. If in the overall ep c.m. the ‘‘current-jet’’ energy  $E_H$  and angle  $\theta_H$  are defined by



then

$$x = \frac{E_H(1 + \cos \theta_H)}{\sqrt{s} - E_H(1 - \cos \theta_H)},$$

$$y = \frac{E_H}{\sqrt{s}}(1 - \cos \theta_H). \quad (14)$$

Assuming that  $\tilde{q}$  decays to  $q + \tilde{G}$ , then  $E_q, \theta_q$  will be interpreted as  $E_H, \theta_H$  and eq. (14) will give a smaller value of  $x$  and  $y$  in  $ep \rightarrow \nu X$  than in genuine  $ep \rightarrow \nu X$  events. In the eq c.m., if  $E_q = \lambda \sqrt{\hat{s}}/2$  we have

$$y = \frac{1}{2}\lambda(1 - \cos \theta), \quad (15)$$

where  $\theta$  is the angle of the scattered quark. For  $eq \rightarrow \nu X$ ,  $\lambda = 1$  and the  $\cos \theta$  and  $y$  distributions are uniform with  $\langle y \rangle \approx \frac{1}{2}$ . In  $eq \rightarrow \nu \tilde{q}, \tilde{q} \rightarrow q \tilde{G}$   $\lambda$  will typically be about  $\frac{1}{2}$  and  $\langle y \rangle$  will be around  $\frac{1}{4}$ . Therefore a cut  $y < \frac{1}{2}$  should enhance  $eq \rightarrow \nu \tilde{q}$  relative to  $eq \rightarrow \nu q$  by a factor of  $O(2)$ . Similarly the apparent  $x$  divided by the true  $x$  (defined as the energy fraction carried by the incident parton) is given by

$$\frac{\lambda(1 + \cos \theta)}{2 - \lambda(1 - \cos \theta)}, \quad (16)$$

which is less than  $\lambda$ , so that a small- $x$  cut will also enhance the signal/noise.

Turning to neutral current processes, we first considered the case  $M_{\tilde{q}} = M_{\tilde{e}} = 40$  GeV,  $M_{\tilde{z}} = 90$  GeV,  $M_{\tilde{\gamma}} = 0$  ignoring the Goldstino contribution, with the results

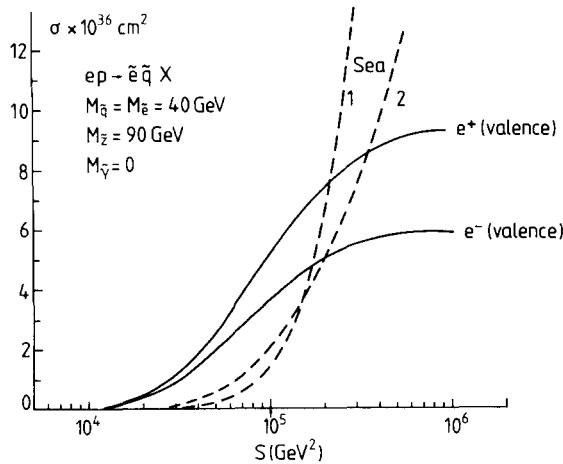


Fig. 2. Cross section for the electroproduction of a scalar electron ( $\tilde{e}$ ) and a scalar quark ( $\tilde{q}$ ) for  $M_{\tilde{e}} = M_{\tilde{q}} = 40$  GeV,  $M_{\tilde{z}} = 90$  GeV,  $M_{\tilde{\gamma}} = 0$ , in the notation of fig. 1.

shown in fig. 2. At  $s = 10^5 \text{ (GeV)}^2$ , the spin averaged cross sections are

$$\begin{aligned}\sigma(e^- \rightarrow \tilde{e}) &= \left(3.7 + \binom{1.4}{2.0}\right) \times 10^{-36} \text{ cm}^2, \\ \sigma(e^+ \rightarrow \tilde{e}^+) &= \left(5.2 + \binom{1.4}{2.0}\right) \times 10^{-36} \text{ cm}^2,\end{aligned}\quad (17)$$

in the notation of eq. (10). For the same  $s$  and  $M_{\tilde{z}}$  but  $M_{\tilde{e}} = M_{\tilde{q}} = 20$ , we found

$$\begin{aligned}\sigma(e^- \rightarrow \tilde{e}^-) &= \left(2.5 + \binom{5.9}{3.1}\right) \times 10^{-35} \text{ cm}^2 \\ \sigma(e^+ \rightarrow \tilde{e}^+) &= \left(2.9 + \binom{5.9}{3.1}\right) \times 10^{-35} \text{ cm}^2\end{aligned}\quad (18)$$

while for the same  $s$  but  $M_{\tilde{e}} = 40 \text{ GeV}$ ,  $M_{\tilde{q}} = 100 \text{ GeV}$ ,  $M_{\tilde{B}} = 60 \text{ GeV}$ ,  $M_{\tilde{W}_3} = 200 \text{ GeV}$ , as might occur in F-type models, we obtained

$$\begin{aligned}\sigma(e^- \rightarrow \tilde{e}^-) &= \left(4.6 + \binom{0.16}{0.42}\right) \times 10^{-37} \text{ cm}^2 \\ \sigma(e^+ \rightarrow \tilde{e}^+) &= \left(1.5 + \binom{0.16}{0.42}\right) \times 10^{-37} \text{ cm}^2.\end{aligned}\quad (19)$$

The approximate relation in eq. (13) may again be used to scale to other masses and energies. If the Goldstino is included with  $A_{ss} = 100 \text{ GeV}$  the cross sections are increased by about 50% e.g. for  $M_{\tilde{z}} = 90$ ,  $M_{\tilde{\gamma}} = 0$ ,  $M_{\tilde{e}} = M_{\tilde{q}} = 40$

$$\begin{aligned}\sigma(e^- \rightarrow \tilde{e}^-) &= \left(6.3 + \binom{1.7}{2.6}\right) \times 10^{-35} \text{ cm}^2, \\ \sigma(e^+ \rightarrow \tilde{e}^+) &= \left(8.1 + \binom{1.7}{2.6}\right) \times 10^{-35} \text{ cm}^2,\end{aligned}\quad (20)$$

For this  $A_{ss}$ , the Goldstino contributes mainly by interference with other terms so its effect behaves roughly as  $A_{ss}^{-4}$  if  $A_{ss}$  is increased.

If  $\tilde{e}$  has exotic decays, cross sections down to  $10^{-36} \text{ cm}^2$  may be detectable. However, if  $\tilde{e} \rightarrow e\tilde{G}$  the events will look like ordinary  $ep \rightarrow eX$  at much lower  $Q^2$  for which the rate is much higher. Nevertheless it should be quite easy to detect  $\tilde{e}$  production using the fact that in ordinary  $ep \rightarrow eX$  the direction and energy of the ‘‘current jet’’ can be predicted from the electron variables in the parton model approximation. In  $ep \rightarrow \tilde{e}\tilde{q}X$ ,  $\tilde{e} \rightarrow e\tilde{G}$ ,  $\tilde{q} \rightarrow q\tilde{G}$  processes the correlation between the electron and the current jet will be very different so that by selecting events in which the characteristics of the current jet differ substantially from those predicted, the signal can be enhanced.

To establish how well this would work in practice, it would be necessary to make a Monte Carlo simulation of a particular experiment. However, by considering the



missing mass  $\Delta M$  and missing transverse momentum  $\Delta p_T$ , which may not be the best variables but can be treated analytically, it seems that it may be possible to detect a threshold for the production of SUSY particles down to the level of a few events per day. In an ordinary deep inelastic even  $\Delta M$  will be zero to the extent that:

- (i) the energy and momentum of all the particles which go through the detector are measured exactly, there being no undetected neutrinos or other neutrals. In this case  $\Delta M$  is the invariant mass of particles which go down the beam pipe;
- (ii) the particles in the beam pipe move exactly parallel (none antiparallel) to the incident proton and have negligible masses.

In practice  $\Delta M$  is not zero but  $\Delta M^2/s$  will be small. For example, if a fraction  $z$  of the energy of the “current jet” in  $ep \rightarrow eX$  is lost the parton model gives

$$\frac{\Delta M^2}{s} = zy(1-x), \quad (21)$$

$y$  is generally small (with a luminosity of  $10^{31} \text{ cm}^{-2} \text{ sec}^{-1}$  90 events/day are expected [17] at HERA with  $y > 0.6$ ,  $x > 0.01$  falling to 0.6 with  $y > 0.6$ ,  $x > 0.2$ , compared to a total of  $1.4 \times 10^4$  with  $x > 0.01$ ,  $y > 0.01$ ). Assuming  $z \leq 0.2$ , there will be almost no events with  $\Delta M^2 > 0.2s$  and few with  $\Delta M^2 > 0.1s$ . Errors in the second assumption are less important if, as is generally believed, particles moving backwards down the beam pipe only extend a few units in rapidity, independent of  $s$ , in which case their contribution to  $\Delta M^2$  is  $O(\sqrt{s})$ . In contrast, typical  $ep \rightarrow \tilde{e}\tilde{q}X$  events will give  $\Delta M^2/s$  of  $O(1/2)$  as can be seen by going to the eq c.m. and using the fact that the typical momentum fraction ( $x_q$ ) of a colliding quark is small compared to one. Thus  $ep \rightarrow \tilde{e}\tilde{q}X$  will produce a threshold for events with substantial  $\Delta M^2/s$  for which there is little background.

A threshold for events with large  $\Delta p_T$  would also provide a signature. If  $M_{\tilde{e}} = M_{\tilde{q}} = M$ , a short calculation gives

$$\langle (\Delta p_T)^2 \rangle = (\tfrac{1}{2}M)^2 \left[ \frac{4}{3} + \frac{2v^2 \langle \sin^2 \alpha \rangle}{1-v^2} \right], \quad (22)$$

where  $v = \sqrt{1 - 4M^2/s}$  is the velocity of the  $\tilde{e}$  and  $\tilde{q}$  and  $\alpha$  is the production angle relative to the beam in the eq c.m. system. In  $eq \rightarrow \tilde{e}\tilde{q}$ ,  $\langle \sin^2 \alpha \rangle$  behaves as  $(\ln s)^{-1}$  for  $s \rightarrow \infty$  so  $\langle (\Delta p_T)^2 \rangle$  grows like  $s/\ln s$ . In ordinary  $ep \rightarrow eX$ ,  $p_T^e = p_T^{\text{hadrons}} = \sqrt{Q^2(1-y)}$  so that at HERA the missing  $p_T$  due to measuring errors will typically be less than 10 GeV. SUSY production should therefore be easy to detect as a threshold for events with large missing transverse momentum\*.

\* Eq. (22) also applies to the SUSY hadroproduction mechanisms discussed in ref. [3]. Generally  $\langle \sin^2 \alpha \rangle$  will be of order  $m^2/s \ln(s/m^2)$ ,  $1/(\ln s/m^2)$ , 1 asymptotically for vector, spinor and scalar exchange respectively (all of which contribute to one or other hadronic production process).  $\langle (\Delta p_T)^2 \rangle$  therefore behaves as  $M^2$ ,  $s/\ln s$  and  $s$  respectively. In any case the missing  $p_T$  is large compared to  $p_T$  lost through measuring errors in ordinary events.

### 3. The supersymmetric content of the nucleon

The distributions  $f_i(x, Q^2)$  for the various species of constituent of the nucleon satisfy evolution equations of the well known form

$$\frac{\partial f_i(x, Q^2)}{\partial \ln Q^2} = \frac{\alpha_s(Q^2)}{2\pi} \sum_j \int_j^1 \frac{dy}{y} P_{ij}\left(\frac{x}{y}\right) f_j(y, Q^2), \quad (23)$$

to leading order in  $\alpha_s$  for  $Q^2$  sufficiently large that  $O(m^2/Q^2)$  mass corrections can be neglected. In addition to the gluon and gluino distributions ( $g(x, Q^2)$ ,  $\tilde{g}(x, Q^2)$ ), there are two singlet distributions for quarks (q) and scalar (s) and pseudoscalar (P) squarks:

$$\begin{aligned} q(x, Q^2) &= \sum_f (q_f + \bar{q}_f), \\ \tilde{q}(x, Q^2) &= \sum_f (s_f + \bar{s}_f + P_f + \bar{P}_f), \end{aligned} \quad (24)$$

and two non-singlet distributions

$$\begin{aligned} q^{\text{NS}}(x, Q^2) &= \sum_f (q_f - \bar{q}_f), \\ \tilde{q}^{\text{NS}}(x, Q^2) &= \sum_f (s_f - \bar{s}_f + P_f - \bar{P}_f). \end{aligned} \quad (25)$$

To leading order in  $\alpha_s$ , momentum conservation implies:

$$\int_0^1 x (q + \tilde{q} + g + \tilde{g}) dx = 1, \quad (26)$$

$$\int_0^1 \sum_i x P_{ij}(x) dx = 0, \quad (27)$$

while quark conservation gives

$$\int_0^1 (q^{\text{NS}} + \tilde{q}^{\text{NS}}) dx = 3, \quad (28)$$

$$\begin{aligned} \int_0^1 dx (P_{qq}(x) + P_{\bar{q}q}(x)) &= 0, \\ \int_0^1 dx (P_{q\bar{q}}(x) + P_{\bar{q}\bar{q}}(x)) &= 0, \end{aligned} \quad (29)$$

We calculated the splitting functions  $P_{ji}$  for  $i \neq j$  and the real (hadronic) bremsstrahlung contribution to  $P_{ii}$  by finding the leading (Weizsäcker–Williams) log to  $O(\alpha_s)$  for deep inelastic scattering on a parton. The virtual contributions can be fixed using the sum rule, eq. (27). Eqs (29) then provide a partial check. As a complete check we also calculated the anomalous dimensions for the momentum

sum rule moment using the operator product expansion. The results are:

$$\begin{aligned}
 P_{qq}(y) &= \frac{4}{3} \left[ \frac{1+y^2}{1-y} - \delta(1-y) \left[ \frac{1}{2} + \int_0^1 \frac{dz}{1-z} (1+z^2) \right] \right], \\
 P_{gq}(y) &= \frac{4}{3} \left[ \frac{1+(1-y)^2}{y} \right], \\
 P_{\bar{q}q}(y) &= \frac{4}{3}y, \\
 P_{\bar{g}q}(y) &= \frac{4}{3}(1-y), \\
 P_{q\bar{q}}(y) &= \frac{4}{3} \left[ \frac{2y}{1-y} - \delta(1-y) \left[ 1 + \int_0^1 \frac{2z}{1-z} dz \right] \right], \\
 P_{g\bar{q}}(y) &= \frac{4}{3} \frac{2(1-y)}{y}, \\
 P_{q\bar{q}}(y) &= P_{\bar{g}\bar{q}}(y) = \frac{4}{3}, \\
 P_{gg}(y) &= 6 \left[ \frac{y}{1-y} + \frac{1-y}{y} + y(1-y), \right. \\
 &\quad \left. - \delta(1-y) \left[ \int_0^1 \frac{z^2 dz}{(1-z)} + \frac{3}{4} + \frac{F}{12} \right] \right], \\
 P_{qg}(y) &= F[(1-y)^2 + y^2], \\
 P_{\bar{q}g}(y) &= F2y(1-y), \\
 P_{\bar{g}g}(y) &= 3[(1-y)^2 + y^2], \\
 P_{\bar{g}\bar{g}}(y) &= 3 \left[ \frac{1+y^2}{1-y} - \delta(1-y) \left[ \int_0^1 dz \frac{1+z^2}{(1-z)} + \frac{F}{6} \right] \right], \\
 P_{g\bar{g}}(y) &= \frac{3[1+(1-y)^2]}{y}, \\
 P_{\bar{q}\bar{g}}(y) &= Fy, \\
 P_{q\bar{g}}(y) &= F(1-y), \tag{30}
 \end{aligned}$$

where  $F$  is the number of flavours. The  $P$ 's should be thought of as distributions with well defined moments, in which the divergences from the  $(1-z)^{-1}$  and  $(1-y)^{-1}$  factors cancel (a suitable infrared cut off should really be introduced before these terms are cancelled).

The pure QCD results can be recovered by setting the  $P$ 's which involve  $\bar{q}$  and  $\bar{g}$  to zero and adjusting the  $\delta$  function contributions in the remaining diagonal  $P$ 's to maintain the sum rules. Likewise the cases that  $m_{\bar{g}}$  is small but  $m_{\bar{q}} \rightarrow \infty$  (which has previously been studied in first [4] and second [5] order in  $\alpha_s$ ) and the  $m_{\bar{q}}$  is

small but  $m_{\tilde{g}} \rightarrow \infty$  can be studied by dropping the irrelevant  $P$ 's and readjusting the remaining diagonal parts.

A final ingredient which is needed to use the evolution equations is the behaviour of  $\alpha_s(Q^2)$ . Writing

$$\frac{\alpha_s(Q^2)}{2\pi} = \frac{B}{\ln(Q^2/\Lambda^2)}, \quad (31)$$

to leading order, we have  $B = 6(33 - 2F)^{-1}$  in ordinary QCD, where  $F$  is the number of flavours, while  $B = 6(33 - 2F - 6 - F)^{-1}$  in SUSY QCD, where  $-6$  and  $-F$  are the contributions of gluinos and scalar plus pseudoscalar quarks respectively.

The evolution equations describe the change of the complete structure functions or more precisely all their moments. We consider first the non-singlet moments

$$\langle \tilde{q}^{(\sim)NS}(Q^2) \rangle \equiv \int_0^1 \tilde{q}^{(\sim)NS}(x, Q^2) dx. \quad (32)$$

The coupled evolution equations show that while  $\langle q^{NS} \rangle + \langle \tilde{q}^{NS} \rangle$  does not evolve, as required by eq. (28), we can form an evolving eigenfunction which satisfies

$$\frac{\partial}{\partial \ln Q^2} [\langle q^{NS} \rangle - 2\langle \tilde{q}^{NS} \rangle] = \frac{-\alpha_s}{\pi} [\langle q^{NS} \rangle - 2\langle \tilde{q}^{NS} \rangle]. \quad (33)$$

Combined with eq. (28) this gives

$$\begin{aligned} \langle q^{NS}(Q^2) \rangle &= 2 + \frac{1}{3}(\langle q^{NS}(Q_0^2) \rangle - 2\langle \tilde{q}^{NS}(Q_0^2) \rangle) \left( \frac{\ln(Q_0^2/\Lambda^2)}{\ln(Q^2/\Lambda^2)} \right)^{2B} \\ \langle \tilde{q}^{NS}(Q^2) \rangle &= 1 - \frac{1}{3}(\langle q^{NS}(Q_0^2) \rangle - 2\langle \tilde{q}^{NS}(Q_0^2) \rangle) \left( \frac{\ln(Q_0^2/\Lambda^2)}{\ln(Q^2/\Lambda^2)} \right)^{2B}. \end{aligned} \quad (34)$$

The asymptotic values are approached quite slowly. For example, if we start with  $\langle \tilde{q}^{NS} \rangle = 0$  at  $Q_0^2 = (50 \text{ GeV})^2$  and then let the numbers of squarks evolve according to massless SUSY QCD, we obtain the results in table 1 for  $\Lambda = 0.2 \text{ GeV}$ .

Next we consider the momentum fractions carried by non-singlet combinations, defining

$$\langle xq(Q^2) \rangle \equiv \int_0^1 xq(x, Q^2) dx, \quad (35)$$

TABLE 1

Net number of quarks and squarks in the nucleon obtained using the asymptotic SUSY QCD evolution equations for  $Q^2 > (50 \text{ GeV})^2$

$Q^2 (\text{GeV})^2$	$(50)^2$	$10^4$	$10^5$	$10^6$	$\infty$
$\langle q^{NS} \rangle$	3	2.85	2.68	2.56	2
$\langle \tilde{q}^{NS} \rangle$	0	0.15	0.32	0.44	1

etc. In ordinary QCD the solution, which is easily obtained, is

$$\begin{aligned}\langle xq(Q^2) \rangle &= \frac{9}{17} + \frac{1}{17} \left( \frac{\ln(Q_0^2/\Lambda^2)}{\ln(Q^2/\Lambda^2)} \right)^{34B/9} (8\langle xq(Q_0^2) \rangle - 9\langle xg(Q_0^2) \rangle), \\ \langle xg(Q^2) \rangle &= \frac{8}{17} - \frac{1}{17} \left( \frac{\ln(Q_0^2/\Lambda^2)}{\ln(Q^2/\Lambda^2)} \right)^{34B/9} (8\langle xq(Q_0^2) \rangle - 9\langle xg(Q_0^2) \rangle),\end{aligned}\quad (36)$$

for the case  $F=6$  (to which we limit ourselves for simplicity). In the case that squarks are infinitely heavy but gluinos are effectively massless we obtain, for  $F=6$ :

$$\begin{aligned}\langle xq(Q^2) \rangle &= \frac{9}{19} - \frac{(d_- + d_+)}{380} + 3 \left( \frac{d_+ - d_-}{380\sqrt{769}} \right), \\ \langle xg(Q^2) \rangle &= \frac{8}{19} + \frac{11(d_+ + d_-)}{3420} + \frac{157(d_+ - d_-)}{3420\sqrt{769}}, \\ \langle x\tilde{g}(Q^2) \rangle &= \frac{2}{19} - \frac{(d_- + d_+)}{1710} - \frac{46(d_+ - d_-)}{855\sqrt{769}},\end{aligned}\quad (37)$$

where

$$\begin{aligned}d_{\pm} &= [-2(47 \mp \sqrt{769})\langle xq(Q_0^2) \rangle \\ &+ 90\langle xg(Q_0^2) \rangle + 9(7 \mp \sqrt{769})\langle x\tilde{g}(Q_0^2) \rangle] \left( \frac{\ln(Q_0^2/\Lambda^2)}{\ln(Q^2/\Lambda^2)} \right)^{-B\lambda_{\pm}},\end{aligned}\quad (38)$$

with

$$\lambda_{\pm} = - \left( \frac{79 \pm \sqrt{769}}{18} \right). \quad (39)$$

In this case  $B = 6(33 - 2F - 6)^{-1}$ . This result was previously derived in ref. [4]. For the case that squarks are effectively massless but gluinos infinitely heavy we obtain the new result (for  $F=6$ ):

$$\begin{aligned}\langle xq(Q^2) \rangle &= \frac{9}{23} - \left( \frac{X_+ + X_-}{92} \right) + \frac{37(X_+ - X_-)}{92\sqrt{817}}, \\ \langle x\tilde{q}(Q^2) \rangle &= \frac{6}{23} - \left( \frac{X_+ + X_-}{138} \right) + \frac{14(X_+ - X_-)}{138\sqrt{817}}, \\ \langle xg(Q^2) \rangle &= \frac{8}{23} + 5 \left( \frac{X_+ + X_-}{276} \right) - \frac{139(X_+ - X_-)}{276\sqrt{817}},\end{aligned}\quad (40)$$

where

$$\begin{aligned}X_{\pm} &= [2(23 \pm \sqrt{817})\langle xq(Q_0^2) \rangle + 18\langle xg(Q_0^2) \rangle \\ &+ 3(-31 \mp \sqrt{817})\langle x\tilde{q}(Q_0^2) \rangle] \left( \frac{\ln Q_0^2/\Lambda^2}{\ln Q^2/\Lambda^2} \right)^{B\lambda_{\pm}},\end{aligned}\quad (41)$$

with

$$\lambda_{\pm} = \frac{55 \mp \sqrt{817}}{18}, \quad (42)$$

and  $B = 6(33 - 2F - F)^{-1}$ . In this and the previous case we have the solution for arbitrary  $F$  but we do not give it as it is very cumbersome. Finally for complete SUSY QCD we have only solved the equations of  $F = 6$  with the results:

$$\begin{aligned} \langle xq(Q^2) \rangle &= \frac{9}{25} + \frac{3P}{25} - \frac{(R+7s)}{810}, \\ \langle x\tilde{q}(Q^2) \rangle &= \frac{6}{25} + \frac{2P}{25} + \frac{(R+7s)}{810}, \\ \langle xg(Q^2) \rangle &= \frac{8}{25} - \frac{4P}{25} + \frac{(4R-53S)}{3645}, \\ \langle x\tilde{g}(Q^2) \rangle &= \frac{2}{25} - \frac{P}{25} - \frac{(4R-53S)}{3645}, \end{aligned} \quad (43)$$

where

$$\begin{aligned} R &= \frac{1}{2}(z_+ + z_-), \quad S = \frac{\frac{1}{2}(z_+ - z_-)}{\sqrt{130}}, \\ z_{\pm}(Q^2) &= [-4(53 \pm 4\sqrt{130})\langle xq(Q_0^2) \rangle + 9(7 \mp \sqrt{130})\langle xg(Q_0^2) \rangle \\ &\quad + 6(53 \pm 4\sqrt{130})\langle x\tilde{q}(Q_0^2) \rangle + 36(-7 \pm \sqrt{130})\langle x\tilde{g}(Q_0^2) \rangle] \\ &\quad \times \left( \frac{\ln(Q_0^2/\Lambda^2)}{\ln(Q^2/\Lambda^2)} \right)^{-B\lambda_{\pm}}, \\ P(Q^2) &= [2\langle xq(Q_0^2) \rangle - 3\langle xg(Q_0^2) \rangle + 2\langle x\tilde{q}(Q_0^2) \rangle - 3\langle x\tilde{g}(Q_0^2) \rangle] \\ &\quad \times \left( \frac{\ln(Q_0^2/\Lambda^2)}{\ln(Q^2/\Lambda^2)} \right)^{5B} \end{aligned} \quad (44)$$

with

$$\lambda_{\pm} = -\frac{50}{9} \pm \frac{2\sqrt{130}}{9}. \quad (45)$$

Eqs (36, 37, 40) and (43) immediately give the asymptotic momentum fractions. These quantities are actually easy to calculate for arbitrary  $F$  even in the general SUSY QCD case and we give the results in table 2 together with numerical values for  $F = 6$ . To see how rapidly these limits are approached we have, rather arbitrarily, assumed that pure QCD holds for  $Q^2 < (50 \text{ GeV})^2$  and that  $\langle xg((50 \text{ GeV})^2) \rangle = \langle xq((50 \text{ GeV})^2) \rangle = 0.5$ . We then consider the following three types of “ $\theta$  function approximation” with the results shown in figs. 3–5:

TABLE 2  
Asymptotic momentum fraction; the arrowed values are for  $F = 6$

	Pure QCD	Gluinos but no squarks	Squarks but no gluinos	SUSY QCD
$\langle xq \rangle$	$\frac{3F}{3F+16} \rightarrow 0.53$	$\frac{3F}{20+3F} \rightarrow 0.47$	$\frac{3F}{16+5F} \rightarrow 0.39$	$\frac{3F}{20+5F} \rightarrow 0.36$
$\langle xg \rangle$	$\frac{16}{3F+16} \rightarrow 0.47$	$\frac{16}{20+3F} \rightarrow 0.42$	$\frac{16}{16+5F} \rightarrow 0.35$	$\frac{16}{20+5F} \rightarrow 0.32$
$\langle x\tilde{q} \rangle$	—	—	$\frac{2F}{16+5F} \rightarrow 0.26$	$\frac{2F}{20+5F} \rightarrow 0.24$
$\langle x\tilde{g} \rangle$	—	$\frac{4}{20+3F} \rightarrow 0.11$	—	$\frac{4}{20+5F} \rightarrow 0.08$

(i) SUSY QCD applies with all masses set to zero for  $\sqrt{Q^2} > 50$  GeV;

(ii) effectively  $M_{\tilde{q}} = \infty$ ,  $M_{\tilde{g}} = 0$  for  $(200 \text{ GeV}) > \sqrt{Q^2} > 50$  GeV but all masses are negligible for higher  $Q^2$ ;

(iii) effectively  $M_{\tilde{g}} = 0$ ,  $M_{\tilde{q}} = \infty$  for  $200 \text{ GeV} > \sqrt{Q^2} > 50$  GeV but all masses are negligible for higher  $Q^2$ .

Figs. 3–5 show that the fraction of momentum in quarks is not much changed by the existence of squarks and gluinos in the  $Q^2$  range accessible to a machine such as HERA ( $Q^2 < \text{few} \times 10^4 (\text{GeV})^2$ ). However squarks could have developed to the point where their presence might be detected by a growth in the longitudinal

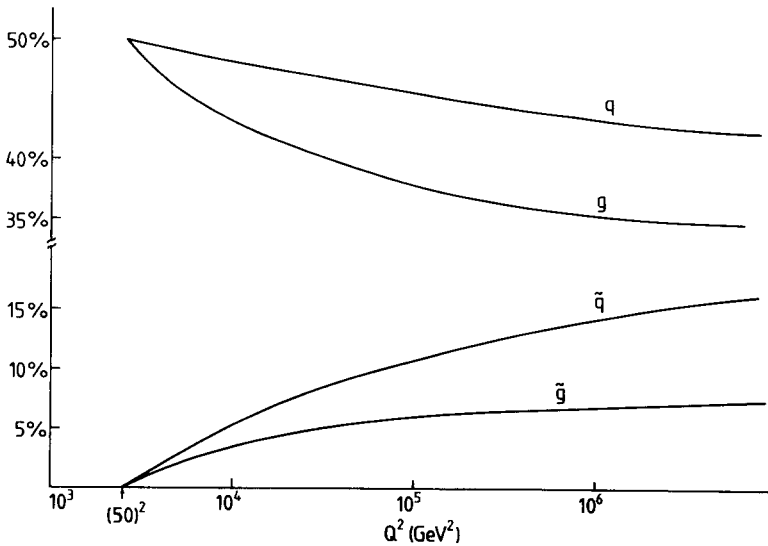


Fig. 3. Evolution of momentum fractions carried by various constituents, as a function of  $Q^2$ , in the  $\theta$  function approximation described in the text in which SUSY particles are switched on at  $Q^2 = (50 \text{ GeV})^2$ .

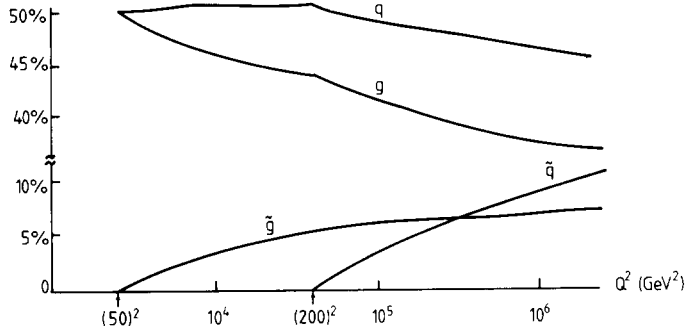


Fig. 4. As for fig. 3 with gluinos switched on at  $(50 \text{ GeV})^2$  and squarks at  $(200 \text{ GeV})^2$ .

cross section. Alternatively we might be able to detect the production of squarks and gluinos directly. To see whether this is feasible we make a more serious treatment of the threshold region in sect. 4 using the fusion model. Fusion calculations of hadroproduction of SUSY particles, which we would expect to be substantial at  $p\bar{p}$  collider energies on the basis of figs. 3–5, have been presented elsewhere [3].

#### 4. Associated production of supersymmetric particles

We treat associated production in the threshold region by folding gluon and quark distributions with the lowest order cross sections for gluon and quark targets, which are given by the following diagrams where  $V$  can be an off-shell  $\gamma$ ,  $Z$ ,  $W^\pm$  or a real  $\gamma$ . As discussed in sect. 7 of ref. [18], and more recently in the second of refs. [3], the use of this “fusion model” of pair production is justified to leading order in  $\alpha_s$  provided  $\alpha_s (|t_{\min}|)$  is small. This condition is satisfied for the EMC data on mu-production of charmed particles [19], except at very small  $x$ , which is

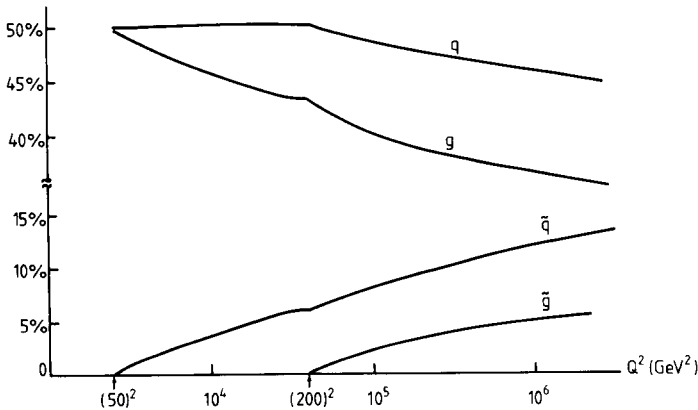
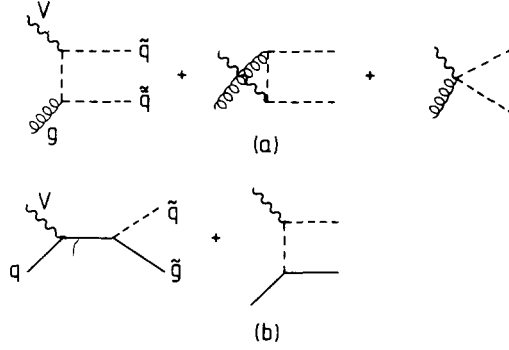


Fig. 5. As for fig. 3 with squarks switched on at  $(50 \text{ GeV})^2$  and gluinos at  $(200 \text{ GeV})^2$ .





described reasonably well by the fusion model. At HERA energies we find that even in photoproduction  $|t_{\min}|$  is greater than  $1 (\text{GeV})^2$  for processes (a) with  $M_{\tilde{q}} > 15 \text{ GeV}$  provided  $x_g x_\gamma < 0.5$ , where  $x_g$  and  $x_\gamma$  are the fraction of the momentum of the proton and electron carried by the gluon and photon respectively. Since  $|t_{\min}|$  increases rapidly for  $Q^2 \neq 0$  and, typically,  $x_{g,q}$  are substantially less than 0.5 (which also increases  $|t_{\min}|$ ) it is probably safe to use the fusion model as a first approximation at HERA energies for  $M_{\tilde{q}} \geq 20 \text{ GeV}$ ,  $M_{\tilde{g}} > \text{few GeV}$ .

We define structure functions in the usual way in terms of the double differential cross section for neutral current production by  $e_{L(R)}^-$  on an unpolarised proton. For neutral current processes

$$\frac{d^2\sigma}{dx dQ^2} = \frac{4\pi\alpha_{e.m.}^2}{Q^4} \frac{1}{x} [xy^2 F_1 + (1-y)F_2 \pm \frac{1}{2}xy(y-2)F_3], \quad (46)$$

and for charged currents

$$\frac{d^2\sigma}{dx dQ^2} = \frac{G_F^2}{2\pi} \left( \frac{M_w^2}{M_w^2 + Q^2} \right)^2 \frac{1}{x} [xy^2 F_1 + (1-y)F_2 \pm \frac{1}{2}xy(y-2)F_3], \quad (47)$$

in a standard notation. Temporarily neglecting Z exchange and putting  $Q_{\tilde{q}} = 1$ , we find for process (a) with V a virtual photon

$$\hat{F}_1 = \frac{\alpha_s}{16\pi\hat{\nu}^2} \left[ \chi(2\hat{s}(2M^2 - Q^2) + 4\hat{\nu}^2) + 4M^2(2Q^2 + 4M^2 - 2\hat{s}) \ln \left( \frac{\sqrt{\hat{s}}}{2M} \right) (1 + \chi) \right],$$

$$\frac{\hat{F}_2}{2\hat{x}} - \hat{F}_1 \equiv \hat{F}_{\text{scalar}} = \frac{\alpha_s}{16\pi} \frac{1}{\hat{\nu}^2} \left[ -6\hat{s}Q^2\chi + 4Q^2(2M^2 + \hat{s}) \ln \left( \frac{\sqrt{\hat{s}}}{2M} \right) (1 + \chi) \right].$$

(48)

where  $\chi = \sqrt{(\hat{s} - 4M^2)/\hat{s}}$ ,  $M$  is the squark mass and  $\hat{\phantom{x}}$  denotes subprocess variables. The real structure functions are then given by

$$f_i^A(x, Q^2) = \rho^A N_G \int_{y_{\min}}^1 dy g(y, Q^2) \hat{f}_i^A\left(\frac{x}{y}, Q^2\right), \quad (49)$$

where  $f$  can be  $F_2$  or  $xF_1$ ,  $y_{\min} = x(4M^2 + Q^2)/Q^2$ ,  $N_G$  is the number of generations of quarks which contribute,  $\rho^{\text{cc}} = 2$  and

$$\rho^{\text{NC}} = \frac{1}{2} \sum_{q=u,d,s=L,R} \left[ Q_e Q_q + \frac{(I_3 - (\sin^2 \theta) Q)_e (I_3 - (\sin^2 \theta) Q)_q}{\sin^2 \theta \cos^2 \theta} \frac{Q^2}{Q^2 + M_z^2} \right]^2. \quad (50)$$

The choice of scale for  $g$  is, of course, somewhat arbitrary as it is nominally irrelevant to leading order in  $\alpha_s$ .

We evaluated eq. (49) as a function of  $Q^2$  for  $x = 0.025$  and  $N_G = 3$  with  $M_{\tilde{q}} = 40$  GeV, using the GHR gluon distribution [14] and the CDHS distribution [20] for comparison. The results are shown in fig. 6. At HERA,  $Q^2$  is bounded by  $2.5 \times 10^3$  GeV<sup>2</sup> for this  $x$ , at which point we obtain for left handed incident electrons:

$$\begin{aligned} F_1^{\text{CC}} &= \begin{pmatrix} 0.17 \\ 0.22 \end{pmatrix}, & F_{\text{scalar}}^{\text{CC}} &= \begin{pmatrix} 0.006 \\ 0.009 \end{pmatrix}, \\ F_1^{\text{NC}} &= \begin{pmatrix} 0.06 \\ 0.07 \end{pmatrix}, & F_{\text{scalar}}^{\text{NC}} &= \begin{pmatrix} 2.2 \times 10^{-3} \\ 3.2 \times 10^{-3} \end{pmatrix}, \end{aligned} \quad (51)$$

where the upper (lower) numbers are for the CDHS gluon distribution [20] (GHR distribution [14]). The  $F^{\text{NC}}$  are smaller by about 30% for right-handed incident electrons. Using the GHR distributions, we find  $F_1^{\text{CC}} = 42$ ,  $F_1^{\text{NC}} = 11.2$  for the background of ordinary leptonproduction events in these conditions. For these masses there is clearly no hope of detecting  $\tilde{q}\tilde{q}$  production through an increase of  $F_1$  or  $F_{\text{scalar}}$ , for which the background is  $O(\alpha_s)$  times  $F_1$  for ordinary events. This

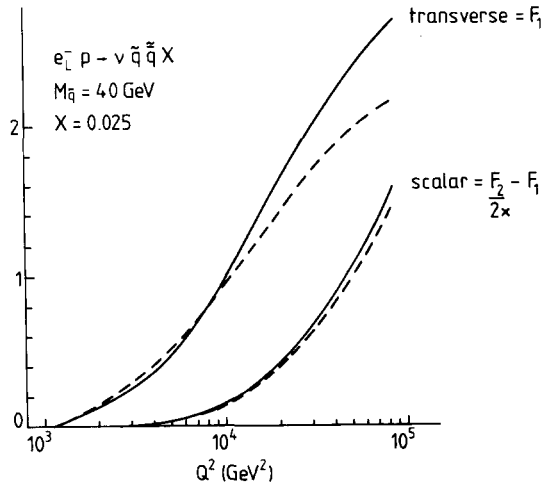


Fig. 6. Contributions to charged current structure functions from  $e^- p \rightarrow \nu \tilde{q} \tilde{q}^* X$  as a function of  $Q^2$  at  $x = 0.025$  for  $M_{\tilde{q}} = 40$  GeV. The solid [dashed] curves were obtained using the CDHS[GHR] gluon distributions.

conclusion is not altered by varying  $x$ . The situation remains hopeless for  $M_{\tilde{q}} = 20$  GeV for which we find (for the same  $x$  and  $Q^2$ ):

$$\begin{aligned} F_1^{\text{CC}} &= \begin{pmatrix} 1.16 \\ 1.08 \end{pmatrix}, & F_{\text{scalar}}^{\text{CC}} &= \begin{pmatrix} 0.18 \\ 0.19 \end{pmatrix}, \\ F_1^{\text{NC}} &= \begin{pmatrix} 0.40 \\ 0.37 \end{pmatrix}, & F_{\text{scalar}}^{\text{NC}} &= \begin{pmatrix} 0.06 \\ 0.07 \end{pmatrix}. \end{aligned} \quad (52)$$

The absolute rate of associated production is very small except for the contribution of almost real photon exchange. We can estimate the large  $Q^2$  contribution by noting that for a luminosity of  $10^{31} \text{ cm}^{-2} \text{ sec}^{-1}$  the rates for ordinary leptonproduction at HERA are expected [17] to be:

Cut	Events/day
$x, y > 0.2$	4
$x > 0.2, y > 0.01$	100
$x > 0.01, y > 0.2$	620
$x, y > 0.01$	$1.4 \times 10^4$ .

It follows from eq. (52) that the rate for  $\tilde{q}\tilde{q}$  production is only of  $O(3\%)$  of these numbers of  $M_{\tilde{q}} = 20$  GeV even at the maximum  $Q^2$ . There is therefore no hope of detecting associated production directly except at small  $Q^2 = xys$ . The low rates at large  $Q^2$  are not surprising in view of the modest rates obtained in sect. 2 for direct eq fusion since the virtual boson in associated production carries only a fraction of the electron energy.

Before turning to photoproduction, we give the cross sections for processes (b). In the case of charged currents, the structure functions for the subprocesses of scattering on a quark (L) or antiquark (R) are given by:

$$\begin{aligned} \hat{x}\hat{F}_1^{\text{L,R}} &= \left[ \hat{x}^2 \frac{\hat{p}^\mu \hat{p}^\nu}{\hat{v}} - \frac{1}{2} \hat{x} g^{\mu\nu} \right] \hat{w}_{\mu\nu} \\ \hat{F}_2^{\text{L,R}} &= \left[ 6\hat{x}^2 \frac{\hat{p}^\mu \hat{p}^\nu}{\hat{v}} - \hat{x} g^{\mu\nu} \right] \hat{w}_{\mu\nu} \\ \hat{F}_3^{\text{L,R}} &= \pm \frac{2\alpha_s}{3\pi\hat{s}\hat{v}^2} [-(2\hat{v}(\mu^2 Q^2 + \hat{s}M^2) - Q^2 \Delta^2)I_{-1} \\ &\quad + (-2\hat{v}(\hat{s} - \Delta) - 2\Delta Q^2 + 2\hat{v}^2 + \hat{v}Q^2 \Delta/\hat{s})I_0 + (\hat{v} - \hat{s})I_1], \end{aligned} \quad (53)$$

where

$$\begin{aligned} g^{\mu\nu} \hat{w}_{\mu\nu} &= \frac{\alpha_s}{6\pi\hat{v}} \left[ -\frac{4}{\hat{s}} I_1 + \frac{4}{\hat{s}^2} (-2\Delta\hat{v} - 2\hat{v}\hat{s} + 3\Delta\hat{s}) I_0 \right. \\ &\quad \left. - \frac{2}{\hat{s}} (Q^2 \hat{s} + 4M^2 \hat{s} - 8\mu^2 \hat{v} + 4\Delta^2) I_{-1} + 2\Delta(4M^2 + Q^2) I_{-2} \right] \end{aligned}$$

$$\frac{\hat{p}^\mu \hat{p}^\nu}{\hat{p}} \hat{w}_{\mu\nu} = \frac{\alpha_s}{6\pi\hat{p}^2} [-2I_1 + (6\Delta - 4\hat{p})I_0 + 2(\hat{p} - \Delta)(3\Delta - \hat{p})I_{-1} + 2\Delta(\hat{p} - \Delta)^2 I_{-2}], \quad (54)$$

with

$$\begin{aligned} I_0 &= \frac{2\hat{p}}{\hat{s}} \chi, \\ I_1 &= \frac{2\hat{p}}{\hat{s}} \left( \Delta - \frac{\hat{p}}{\hat{s}} (\hat{s} + \Delta) \right) \chi, \\ I_{-1} &= \ln \left( \frac{\hat{s}\Delta - \hat{p}(\hat{s} + \Delta) + \hat{p}\chi}{\hat{s}\Delta - \hat{p}(\hat{s} + \Delta) - \hat{p}\chi} \right), \\ I_{-2} &= \frac{2\hat{p}\chi}{(\hat{s}\Delta^2 - 2\Delta\hat{p}(\hat{s} + \Delta) + 4\mu^2\mu^2)}, \\ \chi &= \sqrt{(\hat{s} - M^2 - \mu^2)^2 - 4\mu^2 M^2}. \end{aligned} \quad (55)$$

$\Delta = \mu^2 - M^2$ ,  $\mu$  is the gluino mass and  $M$  the scalar mass. The real ep structure functions are then given by

$$f_i^{\text{CC}}(x, Q^2) = \int dy u(y, Q^2) \hat{f}_i^{\text{u}}\left(\frac{x}{y}, Q^2\right) + \int dy (\bar{d}(y, Q^2) + \bar{s}(y, Q^2)) \hat{f}_i^{\text{R}}\left(\frac{x}{y}, Q^2\right), \quad (56)$$

where  $f_i = F_2$ ,  $xF_1$  or  $xF_3$  and

$$\begin{aligned} f_i^{\text{NC}}(x, Q^2) &= \int dy \sum_i \sum_{s=L,R} \frac{\hat{f}_i^s}{4} q_i(y, Q^2) \\ &\times \left[ Q_e Q_q + \frac{(I_3 - (\sin^2 \theta) Q)_e (I_3 - (\sin^2 \theta) Q)_q}{\sin^2 \theta \cos^2 \theta} \frac{Q^2}{Q^2 + M_z^2} \right]^2, \end{aligned} \quad (57)$$

for  $i = u, d, s, \bar{u}, \bar{d}, \bar{s}$ .

We have evaluated these expressions in the same conditions used for  $\tilde{q}\tilde{q}$  production, i.e.  $x = 0.025$ ,  $Q^2 = 2.5 \times 10^3 \text{ (GeV)}^2$ , with the results:  $M_{\tilde{q}} = 40$ ,  $M_{\tilde{g}} = 20$

$$\begin{aligned} F_1^{\text{CC}} &= \begin{pmatrix} 0.076 \\ 0.072 \end{pmatrix}, & F_{\text{scalar}}^{\text{CC}} &= \begin{pmatrix} 0.014 \\ 0.013 \end{pmatrix}, \\ F_1^{\text{NC}} &= \begin{pmatrix} 0.022 \\ 0.021 \end{pmatrix}, & F_{\text{scalar}}^{\text{NC}} &= \begin{pmatrix} 4.3 \times 10^{-3} \\ 4.0 \times 10^{-3} \end{pmatrix}, \end{aligned} \quad (58)$$

$$M_{\tilde{q}} = 20, M_{\tilde{g}} = 5$$

$$\begin{aligned} F_1^{\text{CC}} &= \begin{pmatrix} 0.29 \\ 0.41 \end{pmatrix}, & F_{\text{scalar}}^{\text{CC}} &= \begin{pmatrix} 0.16 \\ 0.22 \end{pmatrix}, \\ F_1^{\text{NC}} &= \begin{pmatrix} 0.09 \\ 0.12 \end{pmatrix}, & F_{\text{scalar}}^{\text{NC}} &= \begin{pmatrix} 0.05 \\ 0.06 \end{pmatrix}. \end{aligned} \quad (59)$$

Where the upper/lower numbers are for GHR/OR distributions.  $F_3$  is negligibly small at this small  $x$  where the distribution of quarks and antiquarks are almost equal. We see that the rates for  $\tilde{q}\tilde{g}$  production are even smaller than for  $\tilde{q}\tilde{q}$  production. This is because the gluon distribution, which controls the latter process, is much larger than the quark distribution at small  $x$ .

We now concentrate on very small  $Q^2$  electroproduction which provides the only hope of obtaining a measurable rate. The cross section can be estimated using the Weizsäcker–Williams approximation, obtained by taking the small  $Q^2$  limit of the formulae above:

$$\begin{aligned} \sigma_{\text{ep} \rightarrow \text{ex}}(s) &= \int_{Q_{\min}^2}^{Q_{\max}^2} \frac{dQ^2}{Q^2} \frac{\alpha_{\text{e.m.}}}{2\pi} \int \frac{dy}{y} [1 + (1-y)^2] \sigma_{\gamma p \rightarrow x}(s_\gamma = ys), \\ \sigma_{\gamma p \rightarrow x}(s_\gamma) &= \frac{8\pi^2 \alpha_{\text{e.m.}}}{s_\gamma} F_1^{\text{NC}}(\hat{\nu} = \frac{1}{2}s_\gamma, Q^2 = 0), \end{aligned} \quad (60)$$

The real photoproduction cross sections are shown in fig. 7 for  $N_G = 3$  with  $M_{\tilde{q}} = 40$ ,  $M_{\tilde{g}} = 20$ . The corresponding electroproduction cross sections at HERA energies for  $Q_{\min}^2 = m_e^2$ ,  $Q_{\max}^2 = M_\pi^2$  are:

$$\begin{aligned} \sigma(\text{ep} \rightarrow \tilde{q}\tilde{q}) &= \begin{pmatrix} 1.2 \\ 1.4 \end{pmatrix} \times 10^{-36} \text{ cm}^2, \\ \sigma(\text{ep} \rightarrow \tilde{q}\tilde{g}) &= \begin{pmatrix} 9.4 + \begin{pmatrix} 3.4 \\ 3.2 \end{pmatrix} \end{pmatrix} \times 10^{-37} \text{ cm}^2, \end{aligned} \quad (61)$$

where the upper/lower numbers are for CDHS/GHR and OR/GHR distributions, and the valence and sea contributions to  $\tilde{q}\tilde{g}$  production are shown separately. With  $M_{\tilde{q}} = 20$ ,  $M_{\tilde{g}} = 5$  the cross sections for CDHS and GHR distributions are

$$\begin{aligned} \sigma(\text{ep} \rightarrow \tilde{q}\tilde{q}) &= 4.7 \times 10^{-35} \text{ cm}^2, \\ \sigma(\text{ep} \rightarrow \tilde{q}\tilde{g}) &= (11.7 + 10.0) \times 10^{-36} \text{ cm}^2. \end{aligned} \quad (62)$$

The cross sections are increased by a factor of perhaps 2 by the contribution of the rest of the kinematic region.

The rates corresponding to (62) may be observable if there is a clear way to identify the events. With D-type model decays, the only clear signature is the missing  $p_T$  carried off by the Goldstinos in the decays  $\tilde{q} \rightarrow q\tilde{G}$ ,  $\tilde{g} \rightarrow g\tilde{G}$ , or photinos in decays such as  $\tilde{q} \rightarrow q\tilde{\gamma}$  and also  $\tilde{g} \rightarrow \tilde{\gamma}q\bar{q}$ . Since for small  $Q^2$  the virtual photon

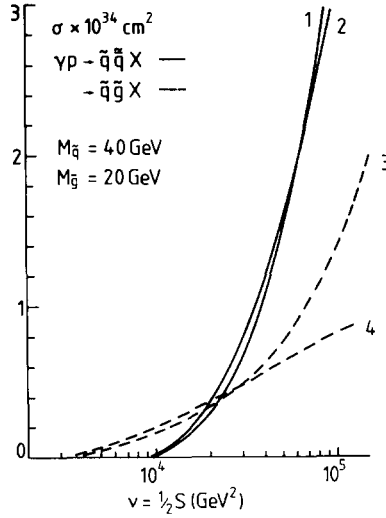


Fig. 7. Cross section for: (a) the photoproduction of  $\tilde{q}$  and  $\tilde{q}$  (solid curves), for  $M_{\tilde{q}} = M_{\tilde{g}} = 40$  GeV, and  $N_G = 3$  with the distributions of '1' CDHS and '2' GHR; (b) the photoproduction of  $\tilde{q}$  and gluino ( $\tilde{g}$ ) (dashed curves) for  $M_{\tilde{q}} = 40$  GeV and  $M_{\tilde{g}} = 20$  GeV, with the distributions of '3' OR and '4' GHR.

Both processes plotted as a function of one half the c.m. energy squared.

momentum is essentially parallel to the electron momentum, we can use eq. (22) in the case of two body decays  $\tilde{q} \rightarrow \tilde{G}q$  and  $\tilde{q} \rightarrow q\tilde{\gamma}$ , noting that  $\langle \sin^2 \alpha \rangle$  remains finite and  $\langle (\Delta p_T)^2 \rangle$  grows for  $s \rightarrow \infty$  in this case. The inclusive cross section for small  $Q^2$  electroproduction of jets with  $p_T > 20$  GeV is of order  $10^{-34}$ – $10^{-33}$  cm<sup>2</sup> at HERA. The background from mismeasurement and from the production of heavy quarks which decay with missing neutrinos may therefore be tolerable. The cross section for charmed quarks with  $p_T > 10$  GeV [20 GeV] is of order  $2 \times 10^{-34}$  cm<sup>2</sup> [ $10^{-35}$  cm<sup>2</sup>] and in any case only about  $\frac{1}{3}$  of the energy on average is taken by the neutrinos in the semileptonic decays.

## 5. Conclusions

The best prospect for detecting supersymmetric particles at HERA seems to be in  $ep \rightarrow e\tilde{q}X$  and  $ep \rightarrow \tilde{\nu}qX$ . A Monte Carlo study would be needed to decide precisely what masses are accessible but our estimates suggest that it should be possible to study the range of masses predicted by models such as Fayet's ( $M_{\tilde{q},\tilde{e}} \lesssim 40$  GeV,  $M_{\tilde{w},\tilde{z}} \approx 80$  GeV). Higher masses could be reached if SUSY particles decay into leptons with appreciable branching ratios, as expected in F-type models in which, however, the masses are expected to be inaccessibly heavy.

Our study of the evolution equations leads to new sum rules for the asymptotic partition of momentum (table 2) and net quark number (eq. (34)). However, the fusion model calculations in sect. 4 show that these asymptotic results are only of

academic interest as far as HERA is concerned. The only realistic possibility of detecting associated production of SUSY particles is in photoproduction, but our calculations show that it will be hard to go much beyond the existing limits on  $M_{\tilde{q}}$  and  $M_{\tilde{g}}$ .

## Appendix

### FEYNMAN RULES FOR MAJORANA PARTICLES

We use a Majorana Representation in which

$$\gamma_\mu^* = -\gamma_\mu, \quad \gamma_0 \gamma_\mu \gamma_0 = -\gamma_\mu^T, \quad (\text{A.1})$$

and the phase of the charge conjugation operation is chosen such that  $\psi^c = \psi^*$ : in terms of four component spinors  $u(k, s) = v^*(k, -s)$  ( $s$  labels spin). We define the  $16\gamma$  matrices:

$$\Gamma_i = \mathbb{1}, i\gamma_5, \gamma_\mu \gamma_5, \gamma_\mu, \sigma_{\mu\nu} = \frac{1}{2}i[\gamma_\mu, \gamma_\nu]$$

so that

$$\gamma_0 \Gamma_i^T \gamma_0 = \eta_i \Gamma_i, \quad (\text{A.2})$$

where  $\eta_i = +1$  for the first  $6\Gamma_i$  and  $-1$  for the last 10. Then the Majorana Field,  $\lambda_M = \lambda_M^*$ , has the plane wave expansion:

$$\begin{aligned} \lambda_M(x) = \int \frac{d^3k}{(2\pi)^3 2k^0} \sum_{\alpha=1,2} [b_\alpha(k) u(\alpha, k) e^{-ik \cdot x} \\ + b_\alpha^+(k) v(-\alpha, k) e^{+ik \cdot x}] \end{aligned} \quad (\text{A.3})$$

and we consider a general lagrangian:

$$\begin{aligned} \mathcal{L} = \frac{1}{2} \bar{\lambda}_a (i \not{\partial} - m_a) \lambda_a + \bar{\psi}_a (i \not{\partial} - M_a) \psi_a \\ + \frac{1}{2} g_{abc}^i \bar{\lambda}_a \Gamma_i \lambda_b \varphi_c + \frac{1}{2} g_{abc}^{i*} \bar{\lambda}_b \Gamma_i \lambda_a \varphi_c^* \\ + k_{abc}^i \bar{\lambda}_a \Gamma_i \psi_b \varphi_c^* + k_{abc}^{i*} \bar{\psi}_b \Gamma_i \lambda_a \varphi_c, \end{aligned} \quad (\text{A.4})$$

where  $\lambda$  and  $\psi$  are Majorana and Dirac fermion fields, respectively;  $\varphi$  are bosonic fields of spin 0 or 1 which may or may not be complex.

Imposing the Majorana condition on  $\lambda$  leads to the constraint:

$$g_{abc}^i = \eta_i g_{bac}^i. \quad (\text{A.5})$$

The Feynman rules can be obtained by the usual Wick expansion, noting that whereas for Dirac fields the only contraction which contributes is  $\langle \psi \bar{\psi} \rangle$ , for Majorana fields the contributing pairs are  $\langle \lambda \bar{\lambda} \rangle$ ,  $\langle \lambda \lambda \rangle$ ,  $\langle \bar{\lambda} \bar{\lambda} \rangle$ .

(i) *Two-point functions.* The two component form for these functions has been given previously in the appendix of ref. [21]. In four component form:

$$\langle O | T[\lambda_\alpha(x) \bar{\lambda}_\beta(y)] | O \rangle = iS(x-y)_{\alpha\beta} \quad (\text{A.6})$$

with

$$S(x-y)_{\alpha\beta} = \int \frac{d^4k}{(2\pi)^4} \frac{(k+m)}{k^2 - m^2 + i\epsilon} e^{-ik \cdot (x-y)},$$

with the diagrammatic representation

$$\beta \bullet \xrightarrow{k} \bullet \alpha \left( \frac{i}{k-m+i\epsilon} \right)_{\alpha\beta}.$$

From (A.6) we obtain the fermion number nonconserving propagators:

$$\langle O | T[\bar{\lambda}_\alpha^T(x) \bar{\lambda}_\beta(y)] | O \rangle = -i\gamma_0 S(x-y)_{\alpha\beta}, \quad (\text{A.7})$$

represented as

$$\beta \bullet \xleftarrow{k} \bullet \alpha \left( -\gamma_0 \frac{i}{k-m+i\epsilon} \right)_{\alpha\beta},$$

and

$$\langle O | T[\lambda_\alpha(x) \lambda_\beta^T(y)] | O \rangle = +iS(x-y) \gamma_{0\alpha\beta},$$

$$\beta \bullet \xrightarrow{k} \bullet \alpha \left( \frac{i}{k-m+i\epsilon} \gamma_0 \right)_{\alpha\beta}, \quad (\text{A.8})$$

where the arrow notation is

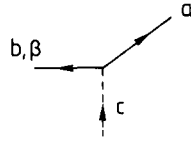
$\bullet \xrightarrow{\quad} \bullet$  denotes  $\lambda$  field to which should be attached  $u(p)[\bar{v}(p)]$  for an incoming [outgoing] state.

$\bullet \xleftarrow{\quad} \bullet$  denotes  $\bar{\lambda}$  field to which should be attached  $v(p)[\bar{u}(p)]$  for incoming [outgoing] state]. For a Majorana field  $u(p) = v^*(p)$ .

(ii) *Three-point functions.* Using the same diagrammatic notation as above we find for the two Majorana fermion-scalar vertex:

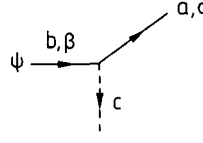
$$\begin{array}{c} \begin{array}{c} \text{a, } \alpha \\ \nearrow \\ \text{b, } \beta \xrightarrow{\quad} \bullet \\ \downarrow \text{c} \end{array} \quad ig_{abc}^i \Gamma_{i\alpha\beta}, \\ \begin{array}{c} \text{a, } \alpha \\ \nearrow \\ \text{b, } \beta \xrightarrow{\quad} \bullet \\ \downarrow \text{c} \end{array} \quad ig_{abc}^i (\gamma^0 \Gamma_i)_{\alpha\beta}, \end{array}$$

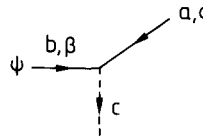




$$ig_{abc}^i (-\Gamma_i \gamma_0)_{\alpha\beta}, \quad (\text{A.9})$$

and for the Majorana-Dirac-scalar vertex:



$$ik_{abc}^i \Gamma_{i\alpha\beta},$$


$$ik_{abc}^i (\gamma^0 \Gamma_i)_{\alpha\beta}, \quad (\text{A.10})$$

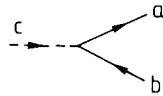
together with diagrams in which the  $\phi$  [and  $\psi$ ] arrow is reversed and  $g^*[k^*]$  is the coupling.

*Closed loops.* A factor of  $\frac{1}{2}$  must be associated with each closed Majorana fermion loop due to the exchange symmetry between the internal lines. This is consistent with the unitarity argument that:

$$\text{Im} \left( \text{wavy line} \text{---} \text{circle with } \lambda \text{---} \text{wavy line} \right) = \sum_{a,b} \left| \text{wavy line} \text{---} \text{triangle with } a, b \text{---} \text{wavy line} \right|^2$$

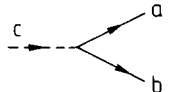
as when summing and integrating over the final states and their momenta a factor of  $\frac{1}{2}$  must be included to avoid double counting.

*Examples.* Decay of a scalar into two Majorana fermions



$$= ig_{abc}^i \bar{u}_a \Gamma_i \nu_b,$$

which can also be written as



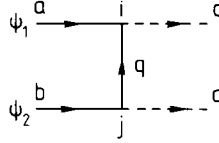
$$= -ig_{abc}^i \bar{u}_a \Gamma_i \gamma_0 \bar{u}_b^T,$$

using (A.2) and (A.5)

$$\begin{aligned} &= -ig_{abc}^i \nu_a^T \gamma_0 \Gamma_i \gamma_0 \bar{u}_b^T = -\eta_i ig_{abc}^i \bar{u}_b \Gamma_i \nu_a \\ &= -ig_{bac}^i \bar{u}_b \Gamma_i \nu_a, \end{aligned}$$

so that if  $a = b$  and the particles have identical momenta the amplitude is zero, as required by Fermi statistics.

As a second example consider the diagrams used in sect. 2:



$$= ik_{ebd}^i (\Gamma_i u_b(2))^T S(q)^T ik_{eac}^i \gamma^0 \Gamma_i u_a(1), \quad (\text{A.11})$$

using (A.1) and (A.2) this reduces to:

$$-\eta i k_{ebd}^i i k_{eac}^i \bar{v}_a(1) \Gamma_i S(q) \Gamma_i u_b(2).$$

Reversing the arrow on the propagator gives

$$ik_{ebd}^i (\gamma^0 \Gamma_i u_b(2))^T S(-q) ik_{eac}^i \Gamma_i u_a(1),$$

using  $\gamma_0^T S(-q) = -S(q)^T \gamma_0$  we recover the original expression (A.11) but with an additional minus sign. This sign can be understood as being due to the exchange of the incoming particles. If the rule with the arrow directed towards  $\psi_a$  corresponds to an initial state  $|a, b\rangle$ , then with the arrow directed towards  $\psi_b$  it corresponds to  $|b, a\rangle = -|a, b\rangle$ . If the cross diagram (scalar momenta and labels exchanged) is added, preserving the arrow convention on the propagator, then the two diagrams will cancel when the incoming fermions have identical momenta and  $a = b$ , as required by Fermi statistics.

## References

- [1] P. Fayet, Ecole Normale preprint LPTENS 82/10, to be published in Proc. 17 Rencontre de Moriond; Talk at the 21st Int. Conf. on High Energy Physics, ed. P. Petiau, M. Porneuf J. de Phys. C-3;  
G.R. Farrar, Rutgers preprint RU-82-3;  
Supersymmetry versus Experiment Workshop, ed. D.V. Nanopoulos, A. Savoy-Navarro and Ch. Tao, CERN TH 3311/EP82/63 CERN;  
C.H. Llewellyn Smith, Oxford preprint 44/82, and other theoretical talks presented at the CERN Supersymmetry Workshop, to be published in Phys. Reports
- [2] G. Barbiellini et al., DESY 79/27
- [3] G.L. Kane and J.P. Leveille, Phys. Lett. 112B (1982) 227;  
P.R. Harrison and C.H. Llewellyn Smith, Nucl. Phys. B213 (1983) 223
- [4] B.A. Campbell, J. Ellis and S. Rudaz, Nucl. Phys. B198 (1982) 1
- [5] I. Antoniadis, C. Kounnas and R. Lacaze, Nucl. Phys. B211 (1983) 216
- [6] P. Salati and J.C. Wallet, Annecy preprint LAPP TH-65 (1982); Nucl. Phys. B209 (1982) 389
- [7] H.J. Behrend et al., CELLO collaboration, Phys. Lett 114B (1982) 287;  
W. Bartel et al., JADE collaboration, Phys. Lett 114B (1982) 211;  
B. Adeva et al., Mark J Collaboration, Phys. Lett. 115B (1982) 345;  
R. Brandelik et al., TASSO collaboration, Phys. Lett. 113B (1982) 499
- [8] P. Fayet, Phys. Lett. 69B (1977) 489;  
S. Weinberg, Phys. Rev. D26 (1982) 287;  
R. Barbieri, S. Ferrara and D.V. Nanopoulos, Z. Phys. C13 (1982) 267; Phys. Lett. 116B (1982) 16;  
L.J. Hall and I. Hinchliffe, Phys. Lett. 112B (1982) 351

- [9] L.I. Ibáñez and G.G. Ross, Phys. Lett. 58B (1982) 67;  
J.R. Ellis, L.I. Ibáñez and G.G. Ross, Phys. Lett. 113B (1982) 283;  
M. Dine and W. Fischler, Phys. Lett. 110B (1982) 227;  
L. Alvarez-Gaumé, M. Claudson and M.B. Wise, Nucl. Phys. B207 (1982) 96  
G.R. Nappi and B.A. Ovrut, Phys. Lett. 113B (1982) 175;  
M. Dine and W. Fischler, Nucl. Phys. B204 (1982) 346
- [10] J. R. Ellis and G.G. Ross, Phys. Lett. 117B (1982) 397
- [11] M. Suzuki, Phys. Lett. 115B (1982) 40;  
M.J. Duncan, Nucl. Phys. B214 (1983) 21
- [12] P. Fayet, in Unification of the fundamental interactions (1980) ed S. Ferrara, J.R. Ellis and P van Nieuwenhuizen (Plenum, New York)
- [13] M. Fukugita and N. Sakai, Phys. Lett. 114B (1982) 23
- [14] M. Glück, E. Hoffman and E. Reya, Z. Phys. C13 (1982) 119
- [15] J.F. Owens and E. Reya, Phys. Rev. D17 (1978) 3003
- [16] B.H. Wiik in DESY HERA 81/18
- [17] ECFA 80/42 – DESY HERA 80/01, part 2
- [18] A.B. Carter and C.H. Llewellyn Smith, Nucl. Phys. 162B (1980) 397
- [19] J.J. Aubert et al., Phys. Lett. 110B (1982) 73
- [20] H. Abramowicz et al., Z. Phys. C12 (1982) 289
- [21] J. Schechter and J.W.F. Valle, Phys. Rev. D24 (1981) 1883